Foxc2 enhances proliferation and inhibits apoptosis through activating Akt/mTORC1 signaling pathway in mouse preadipocytes

Lu Gan,[1] Zhenjiang Liu,[1] Wei Jin, Zhongjie Zhou, and Chao Sun[2]

College of Animal Science and Technology, Northwest A&F University, Yangling, Shaanxi 712100, China

Abstract **Forkhead box C2 (Foxc2) protein is a transcription factor in regulation of development, metabolism, and immunology. However, the regulatory mechanisms of Foxc2 on proliferation and apoptosis of preadipocytes are unclear. In this study, we found that high-fat-diet-induced obesity elevated the expression of Foxc2 and cyclin E after 6 weeks. Additionally, Foxc2 suppressed preadipocyte differentiation, increased cell counts and augmented G1-S transition of preadipocytes, along with the elevation of cyclin E expression and the reduction levels of p27 and p53. Furthermore, Foxc2 knockdown reduced early apoptotic cells with accompanying reduction of mitochondrial membrane potential and increased fragmentation of genomic DNA. We show that Foxc2 reduces the expression of Bax, caspase-9, and caspase-3 in both serum-starved and palmitic acid-induced cell apoptotic models, which confirms the anti-apoptotic role of Foxc2. Moreover, the protein kinase B (Akt)/mammalian target of rapamycin (mTOR)C1 signaling pathway and the ERK/mTORC1 signaling pathway were activated along with preadipocyte proliferation in response to Foxc2 overexpression, whereas apoptosis marker genes were downregulated during this process. Those effects were blocked by the interference of Foxc2 or signal pathways specific inhibitors.** **These data collectively reveal that Foxc2 enhances proliferation of preadipocytes and inhibits apoptosis of preadipocytes by activating the Akt/mTORC1 and ERK/mTORC1 signaling pathways.**—Gan, L., Z. Liu, W. Jin, Z. Zhou, and C. Sun. **Foxc2 enhances proliferation and inhibits apoptosis through activating Akt/mTORC1 signaling pathway in mouse preadipocytes.** ***J. Lipid Res.*** **2015.** 56: **1471–1480.**

Supplementary key words forkhead box C2 • transcription factor • cell death • fat • cell signaling • protein kinase B/mammalian target of rapamycin C1 signaling pathway

Forkhead box C2 (Foxc2) protein is a member of the forkhead/winged helix transcription factor family and is found in various organs and tissues, such as the cardiac system, mammary gland, liver, and adipose tissue. In general, Foxc2 plays important roles in the regulation of cell growth, proliferation, differentiation, apoptosis, and energy metabolism. Mice lacking Foxc2 die during embryogenesis or perinatally and exhibit aortic arch and skeletal defects (1–4). Previous studies have shown that, in adipocytes, either a high-calorie diet or insulin induces Foxc2 expression, suggesting that Foxc2 is an important metabolic regulator of mitochondrial morphology and metabolism (5, 6). In 3T3-L1 preadipocytes, Foxc2 extensively decreased the expression of CCAAT/enhancer-binding protein α (C/EBPα), PPARγ, adiponectin, perilipin, and adipocyte protein 2 (aP2), so as to prevent preadipocytes from differentiating into mature adipocytes with lipid droplets (7). Recent studies mostly focus on the regulation role of Foxc2 on trans-differentiation of intra-abdominal white adipose tissue to brown fat-like tissue in transgenic mice that overexpress Foxc2, and those mice that present a lean and insulin-sensitive phenotype and are able to counteract metabolic disorders associated with obesity, including type 2 diabetes and hyperlipidemia (6, 8). The Foxc2 level could be increased by a high-fat diet (HFD), which counteracted most of the symptoms associated with obesity, including hypertriglyceridemia and diet-induced insulin resistance, and these results suggest a potentially therapeutic role of Foxc2 in the protection against type 2 diabetes (6, 9–13).

Foxc2 plays an important role in cell proliferation (14). Research on the regulatory role of Foxc2 in muscle regeneration and osteogenesis has shown that downregulation of endogenous Foxc2 expression in undifferentiated C2C12 myoblasts decreases cell proliferation, whereas forced expression of Foxc2 enhanced myoblast proliferation

This work was supported by grants from the Major National Scientific Research Projects (2015CB943102) and the National Nature Science Foundation of China (31172185).

Manuscript received 13 January 2015 and in revised form 12 June 2015.

Published, JLR Papers in Press, June 25, 2015
DOI 10.1194/jlr.M057679

Abbreviations: Akt, protein kinase B; CCK-8, Cell Counting Kit-8; Foxc2, forkhead box C2; HFD, high-fat diet; mTOR, mammalian target of rapamycin; PI, propidium iodide; S6K1, ribosomal protein S6 kinase polypeptide 1.

[1] L. Gan and Z. Liu contributed equally to this work.
[2] To whom correspondence should be addressed.
e-mail: sunchao2775@163.com

and delayed cell-cycle withdrawal and apoptosis, as well as inhibited myotube formation (15, 16). However, there are few reports on the relationship between Foxc2 and apoptosis of cells. Some studies have found that overexpression of Foxc2 increased both cell viability and cell number, whereas interference of Foxc2 has opposite effects on MC3T3-E1 cells and primary caldaria cells of mice; Foxc2 interference induced an arrest of the G0/G1 phase of the cell cycle along with a reduction of phosphorylation of both protein kinase B (Akt) and mammalian target of rapamycin (mTOR) signaling pathways (17). The mTOR signaling cascades play an important role in both the survival and proliferation of tumor cells. Kim et al. (18) found that embelin suppressed the constitutive activation of the Akt/mTOR signaling cascade, which correlated with the induction of apoptosis in prostate cancer cells of humans. The Akt/mTOR signaling cascade has diversified functions on cell proliferation; Akt is the key upstream molecule that links the ligation of growth factor receptors to the phosphorylation and activation state of mTOR (19, 20). The ERK pathway is involved in various cell types by activating a series of protein kinases and, downstream, targets phosphorylation in cellular events such as cell proliferation, differentiation, survival, and motility (21, 22).

This study aimed to investigate the regulatory mechanism of Foxc2 in the proliferation and apoptotic process on preadipocytes. To do so, we enhanced the Foxc2 gene expression in preadipocytes and found that the overexpression of Foxc2 enhanced cell proliferation and inhibited cell apoptosis, and then the Akt and ERK1/2 signaling pathways were activated, which in turn activated downstream mTORC1 pathway. The results imply that manipulating Foxc2 could offer a new theoretical means to prevent and treat obesity and type 2 diabetes.

MATERIALS AND METHODS

Animal experiments

Two-week-old Kunming male mice were purchased from the Laboratory Animal Center of the Fourth Military Medical University. All mice were treated in accordance with the applicable guidelines and regulations approved by the Animal Ethics Committee of Northwest A&F University. They were allowed ad libitum access to water and standard chow laboratory diet for the first 2 weeks to allow them to adjust to the new environment. Mice were subsequently randomly assigned to two groups: an HFD-fed group (87.5% chow diet + 10% lard + 2% cholesterol + 0.5% bile salt; Animal Center of the Fourth Military Medical University) or a chow diet-fed group (Animal Center of the Fourth Military Medical University) for the next 10 weeks. The animal room was maintained under controlled conditions of temperature at 25 ± 1°C, humidity at 55 ± 5%, and a 12 h light/12 h dark cycle. Body weight was recorded once a week.

Cell culture

Epididymal white adipose tissues were harvested, visible fibers and blood vessels were removed, and the adipose tissue was washed three times with PBS buffer containing 200 U/ml penicillin (Sigma, St. Louis, MO) and 200 U/ml streptomycin (Sigma). Then the adipose tissue was minced into fine sections (1 mm^3) with scissors and incubated in 10 ml of digestion buffer containing DMEM/F-12 (Gibco), 100 mM HEPES (Sigma), 1.5% BSA (Sigma), and 2 mg/ml type I collagenase (Sigma) for 50 min at 37°C in a water bath. After the incubation, growth medium [DMEM/F-12 (50:50)], 10% fetal bovine serum (Sigma), 100 U/ml penicillin, and 100 U/ml streptomycin were added to the digestion flask. Flask contents were mixed and filtered through nylon screens with 250 μm and 20 μm mesh openings to remove undigested tissue and large cell aggregates. The filtered cells were centrifuged at 300 *g* for 7 min at room temperature to separate floating adipocytes from cell pellets. Isolated cell pellets were suspended in DMEM/F12 (Invitrogen). Finally, cells were seeded into 35 mm primary culture dishes at a density of 8×10^4 cells/dish and incubated at 37°C under a humidified atmosphere of 5% CO_2 and 95% air until confluence. The medium was changed every other day.

Transfection of adipocyte with Foxc2 shRNA plasmid and Foxc2 overexpressed plasmid

Foxc2 expression plasmid vector pcDNA-Foxc2 was kept in our lab. shRNA sequence against Foxc2 was contrived and synthesized by GenePharma Company (Shanghai, China) using pGPU6/Neo shRNA expression vector, named shRNA-Foxc2. Two micrograms of interference or expression plasmid's DNA were mixed with 2 μl X-tremeGENE HP reagent (Roche, Switzerland) and Opti-MEM I media (Invitrogen) and then added into the culture dish. The interference efficiency and overexpression efficiency were determined using Western blot 48 h after the transfection.

Cell proliferation assay

Cell proliferation was measured using Cell Counting Kit-8 (CCK-8) (Vazyme, China) assay. The transfected cells were first seeded in a 96-well plate at a density of 2×10^3 for 12 h; then 10 μl CCK-8 solution was added into each well and incubated further for 1 h at 37°C. Absorbance was quantified at 450 nm using Vector 5 (Bio-Tech Instruments, USA).

Cell cycle assay

Cultured cells were harvested using trypsin/EDTA and washed twice with PBS buffer. Aliquots of 2×10^6 cells were centrifuged at 1,500 *g* for 5 min, precipitants of cells were fixed in 70% ethanol and stained with 500 μl propidium iodide (PI) solution (100 μg/ml RNase and 50 μg/ml PI in 1× PBS buffer). Percentages of cells within cell cycle compartments (G0/G1, S, and G2/M) were determined by BD FACScan (BD Biosciences, Franklin Lakes, NJ) and data were analyzed using Cell Quest software (BD Biosciences).

Apoptosis assessment

The TUNEL assay was performed using an in situ cell death detection kit (Roche, Switzerland). Mouse preadipocytes were grown to 60% confluence on a 60 mm culture dish and the Foxc2 reconstructed plasmid was transfected into cells with X-treme GENE HP. After a 48 h transfection, the cell suspension was then added with 4% (v/v) paraformaldehyde in PBS buffer to fix the cells for 30 min at room temperature. Cells were permeabilized with 0.1% Triton X-100 on ice for 2 min and then stained by TUNEL fluorochrome. The areas of cells stained with TUNEL were measured using Image-Pro Plus analyzer (Palmerton, Inc.). Then images of cells were obtained using inverted fluorescent microscopy.

Apoptosis was also determined by FITC-labeled annexin V/PI double staining and flow cytometry analysis. An annexin V-FITC apoptosis assay kit (Vazyme, Piscataway, NJ) was used according

to the manufacturer's protocol. Only fluorescein-positive cells without PI staining were regarded as apoptotic cells, and the percentages were determined by flow cytometry (BD FACScan; BD Biosciences) and data were analyzed using Cell Quest software (BD Biosciences).

Mitochondrial membrane potential measurement

Fluorescent probe JC-1 (Beyotime, China) was used to estimate mitochondrial membrane potential ($\Delta\Psi m$). Cells were incubated with 5 μg/ml JC-1 at 37°C for 10 min, then washed twice with PBS and placed in fresh medium without serum. Images were scanned using a fluorescence microscope (Nikon TE2000-U, Japan). Cells were also gently harvested with trypsin and transferred on ice for measurement using a flow cytometer. JC-1 was excited at 488 nm and the monomer signal (green) was recorded at 525 nm (JC-1 monomer) in a minimum of 10,000 cells per sample. Simultaneously, aggregate signal (red) was recorded at 590 nm (JC-1 aggregates). The ratio of red/green fluorescent intensity was then calculated.

Immunoblot analysis

Mouse preadipocytes were solubilized in adipocyte lysis buffer. The solubilization proceeded for 40 min at 4°C, then the solution was centrifuged at 12,000 *g* for 15 min at 4°C and the supernatants were used for determination of protein concentration. In addition, protein samples (30 μg) were separated by electrophoresis on 12% and 5% SDS-PAGE gels using slab gel apparatus, and transferred to PVDF nitrocellulose membranes (Millipore, USA) blocked with 5% skim milk powder /Tween 20/TBST at room temperature for 2 h. The membranes were then incubated with primary antibodies against Foxc2, p53, p27, cyclin E, Bax, Bcl-2, caspase-9, cleaved caspase-9, caspase-3, cleaved caspase-3, FoxO3a, phospho-FoxO3a, raptor, β-actin (Bioworld, China), IRS1, phospho-IRS1 (T896), Akt, phospho-Akt (Ser473), mTOR, phospho-mTOR (Ser2448), ribosomal protein S6 kinase polypeptide 1 (S6K1), phospho-S6K1 (Thr389) (Epitomics), ERK1/2, and phospho-ERK1/2 (Thr202/Tyr204, Thr185/Tyr187) (Abcam, USA) at 4°C overnight. Akt phosphorylation-specific inhibitor MK-2206, ERK phosphorylation-specific inhibitor U0126, and mTORC1 inhibitor rapamycin were purchased from Selleck Chemical (USA). Following this step, the appropriate HRP-conjugated secondary antibodies (Boaoshen, China) were added in and incubated for 2 h at room temperature. Proteins were visualized using chemiluminescent peroxidase substrate (Millipore), and then the blots were quantified using ChemiDoc XRS system (Bio-Rad, USA).

Statistical analysis

Statistical calculations were performed with SAS v8.0 (SAS Institute, Cary, NC). The effects of the treatments were determined using the one-way ANOVA procedure. Comparisons among the means of individual treatments were made by Fisher's least significant difference (LSD) post hoc test once the ANOVA analysis showed a significant effect of the treatments. Data are presented as mean ± SD, and $P < 0.05$ was considered to be significant.

RESULTS

Foxc2 inhibited mouse preadipocyte differentiation and increased cell counts

To study the effects of HFD on Foxc2, we placed 2-week-old male mice on a HFD. Body weight increased significantly during the 10 weeks of HFD feeding ($P < 0.05$), while there was no difference in food intake (**Fig. 1A, B**). Foxc2 expression elevated during the last 4 weeks, accompanied by increased cyclin E mRNA expression ($P < 0.05$) (Fig. 1C, D). To further analyze the function of Foxc2, we used forced gene expression detection in mouse preadipocytes. Compared with the control group, the expression of Foxc2 increased significantly in the pcDNA-Foxc2 group ($P < 0.01$), while it decreased in the shRNA-Foxc2 group ($P < 0.01$) (Fig. 1E). We next analyzed the significance of Foxc2 in preadipocyte differentiation. Figure 1F, G shows that forced expression of Foxc2 blocked preadipocyte differentiation along with decreasing the levels of PPARγ and HSL. In addition, Foxc2 enhanced the rate of cell counts while serum-starved treatment did not alter the proliferation status of preadipocytes ($P < 0.05$) (Fig. 1H, I). Taken together, these discoveries suggest that Foxc2 has impacts on preadipocyte proliferation.

Foxc2 enhanced preadipocyte proliferation and induced cell cycle transition

The CCK-8 cell proliferation assay demonstrated an enhanced rate of proliferation in the pcDNA-Foxc2 group compared with that in the control group and the shRNA-Foxc2 group (Fig. 1H). To determine whether Foxc2 regulated preadipocyte cell cycle, cells were subjected to cell-cycle analysis by fluorescence-activated cell sorter. A lower percentage of pcDNA-Foxc2 cells underwent G1 arrest after Foxc2 forced expression compared with shRNA-Foxc2 cells (**Fig. 2A**). This finding was confirmed by the decreased p27 level observed in pcDNA-Foxc2 cells (Fig. 2B). Furthermore, p53 functions to prevent initiation of DNA replication in the G1/S checkpoint and maintains G0/G1 arrest. Indeed, data from Western blots demonstrated that p53 (Fig. 2B) was downregulated in the forced expression Foxc2 group ($P < 0.05$), while it was upregulated after Foxc2 stable knockdown in the normal growth medium. The slight decrease in G2 arrest that we observed in pcDNA-Foxc2 cells showed that a higher proportion of pcDNA-Foxc2 cells underwent a transition from G1-phase to S-phase (Fig. 2A). As expected, cyclin E expression increased markedly in the pcDNA-Foxc2 group ($P < 0.05$) (Fig. 2B). The protein levels of p27, p53, and cyclin E showed the same results after being cultured in the serum-starved medium for 6 h (Fig. 2C), which confirmed that starvation did not change the role of Foxc2 in regulating proliferation of preadipocytes.

Foxc2 inhibited preadipocyte apoptosis

Mitochondria play a vital role as gatekeepers of apoptosis. In addition, mitochondrial membrane potential is an important parameter of mitochondrial function and an indicator of apoptosis (23). JC-1 staining was used to detect the mitochondrial membrane potential after transfection with Foxc2. As shown in **Fig. 3A**, pcDNA-Foxc2 increased ($P < 0.01$) red fluorescence intensity. Flow cytometry analysis showed that the overexpression of Foxc2 increased ($P < 0.01$) the ratio of the red/green light by 50%, while stable knockdown of Foxc2 decreased ($P < 0.01$)

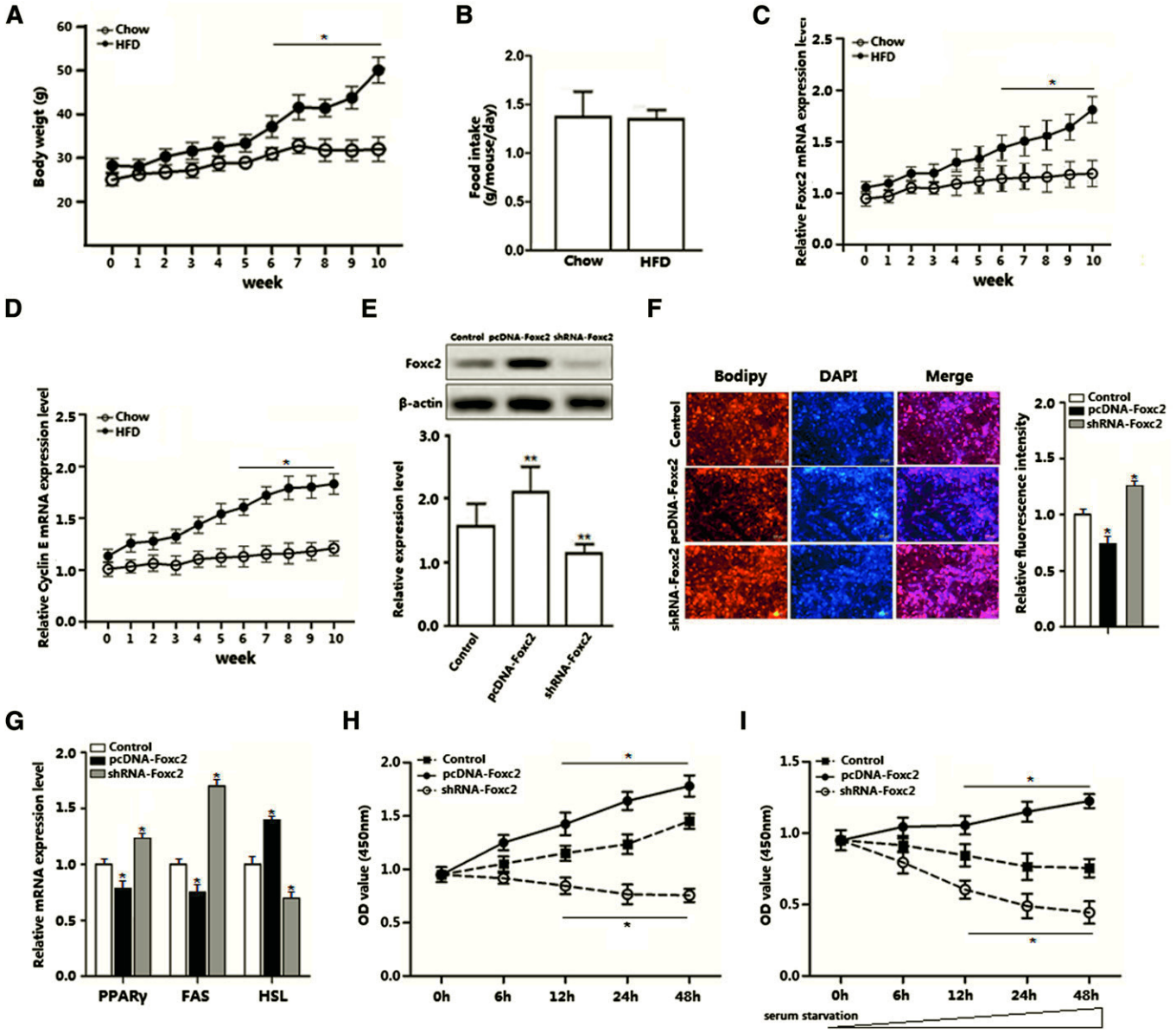

Fig. 1. Foxc2 inhibited mouse preadipocyte differentiation and increased cell counts. A: Body weight of male mice fed a HFD (n = 18 each). B: Food intake of male mice fed a HFD and a chow diet (n = 18 each). C: Relative Foxc2 mRNA expression in both chow diet and HFD groups (n = 18 each). D: Relative cyclin E mRNA expression in both chow diet and HFD groups (n = 18 each). E: Transfection efficiencies of overexpression Foxc2 (pcDNA-Foxc2) and shRNA-Foxc2 in mouse preadipocytes (n = 3). F: BODIPY staining of differentiation preadipocytes after transfection with pcDNA-Foxc2 and shRNA-Foxc2 for 48 h (n = 3). G: Relative mRNA expression of PPARγ, FAS, and HSL after transfection with pcDNA-Foxc2 and shRNA-Foxc2 for 48 h (n = 3). H: Cell counting after cells were cultured for 6, 12, 24, and 48 h in groups: control group, pcDNA-Foxc2 group, and shRNA-Foxc2 group (n = 3 each). I: Cell counting after serum-starved cells were cultured for 6, 12, 24, and 48 h in groups: control group, pcDNA-Foxc2 group, and shRNA-Foxc2 group (n = 3 each).Values are mean ± SD. *$P < 0.05$, **$P < 0.01$ compared with the control.

the red/green ratio (Fig. 3B). Therefore, Foxc2 was capable of maintaining the mitochondrial membrane potential and preventing the cells from early apoptosis. Additional evidence for Foxc2 reduction of apoptosis was provided by annexin V/PI staining, demonstrating that forced expression of Foxc2 attenuated the rate of preadipocyte apoptosis (Fig. 3D). During the later stage of apoptosis, some kinds of DNase are activated and cut genome DNA in the nucleus into fragments that can be detected by TUNEL staining. As shown in Fig. 3C, Foxc2 knockdown resulted in a higher number of TUNEL-positive cells compared with the control group ($P < 0.05$). This verified the anti-apoptotic role of Foxc2. The expression of apoptosis marker genes, Bax, cleaved caspase-3, and cleaved caspase-9, were all decreased ($P < 0.01$) in the pcDNA-Foxc2 group (Fig. 3E). Taken together, these findings indicated that Foxc2 affects cell survival and attenuates cell apoptosis.

Foxc2 attenuated serum-starved and palmitate-induced preadipocyte apoptosis

Palmitic acid had been shown to induce apoptosis in adipocytes (8, 24–26). To verify the role of Foxc2 during

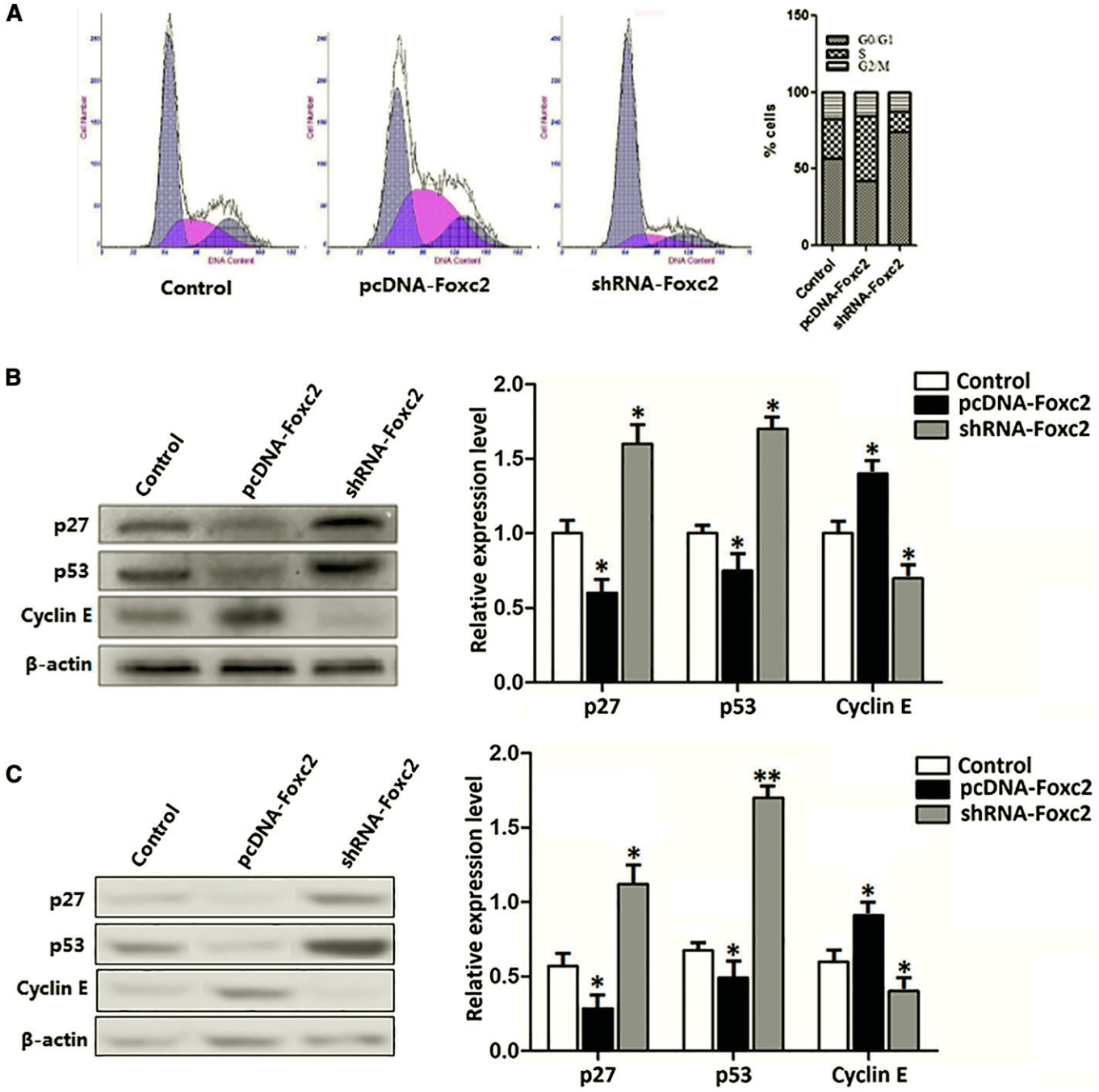

Fig. 2. Foxc2 enhanced preadipocyte proliferation and induced cell cycle transition. Mouse preadipocytes were pretreated with either pcDNA-Foxc2 or shRNA-Foxc2 plasmids. A: Cell cycle analyzed in flow cytometry and the percentages of cell counts at different phases (n = 3). B: The protein levels of p27, p53, cyclin E, and β-actin in normal growth medium (n = 3). C: The protein expression levels of p27, p53, cyclin E, and β-actin in serum-starved medium for 6 h (n = 3). The total β-actin was used as the loading control. Values are mean ± SD. *$P < 0.05$, **$P < 0.01$ compared with the control.

this process, 0.2 mM palmitic acid was used to stimulate mouse preadipocytes for 24 h to trigger apoptosis. The treatment with palmitic acid increased the expression of Bcl-2 ($P < 0.05$), but reduced expression of Bax ($P < 0.05$), cleaved caspase-9 ($P < 0.05$), and cleaved caspase-3 ($P < 0.05$), as shown in **Fig. 4A**; so palmitic acid induced cell apoptosis successfully. With the expression of Foxc2, cell apoptosis was attenuated significantly (Fig. 4A). Similarly, expression of Foxc2 protected against starvation-induced apoptosis (Fig. 4B). The reduction of serum-starved and palmitate-induced apoptosis in mouse preadipocytes further confirmed that Foxc2 had a negative effect on cell apoptosis.

Foxc2 regulated proliferation and apoptosis of preadipocytes via the mTORC1 pathway

We next explored possible molecular mechanisms underlying Foxc2 regulation of proliferation and apoptosis

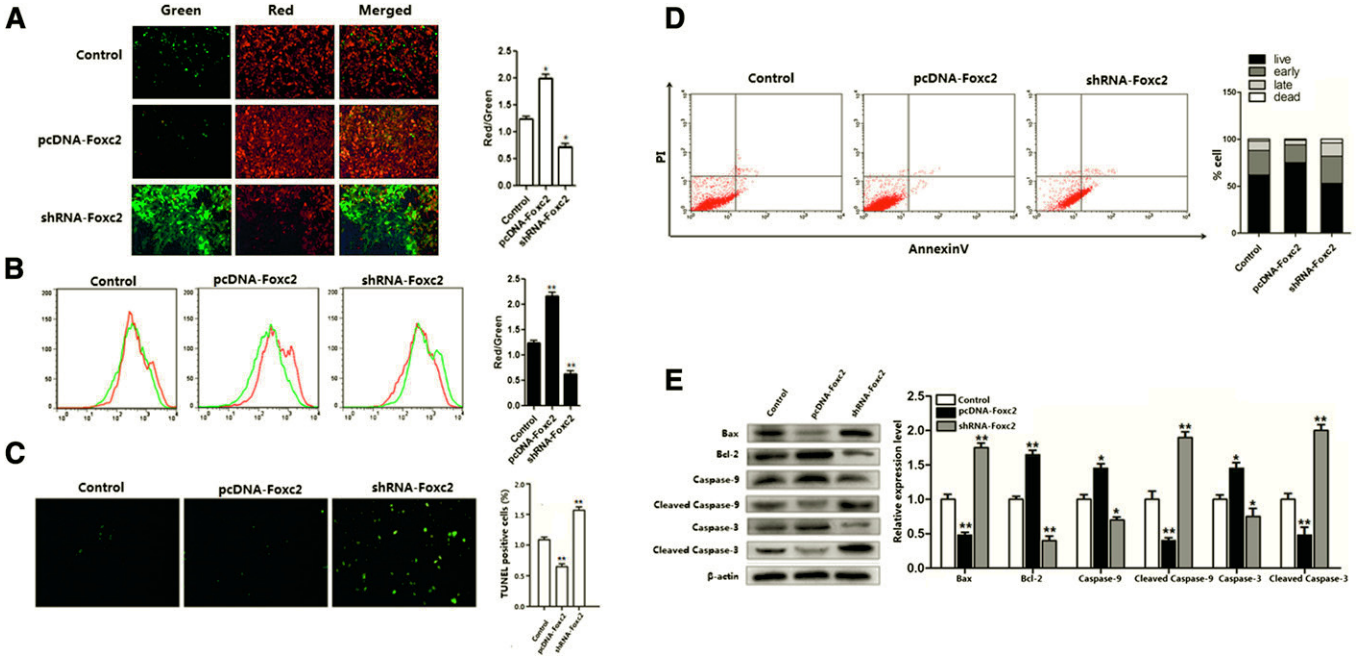

Fig. 3. Foxc2 inhibited preadipocyte apoptosis. Mouse preadipocytes were pretreated with either pcDNA-Foxc2 or shRNA-Foxc2 plasmids. A: Images of mitochondrial membrane integrity under fluorescence microscope after dyeing with JC-1. Scale bar: 100 μm (n = 3). B: Cell counts by flow cytometry after staining with JC-1. The shift of green and red fluorescence intensities were quantitated by subtracting the mean of treated cultures from the mean of the control. The ratio of red/green fluorescence intensity was then used to quantitate the potential of mitochondrial membrane (n = 3). C: Images of preadipocyte apoptosis under fluorescence microscope after TUNEL staining. Fluorescence intensity was used to quantitate the TUNEL-positive cells. Scale bar: 100 μm (n = 3). D: Annexin V/PI staining analysis of apoptosis. The apoptotic rates were determined by flow cytometry (n = 3). E: Protein expressions of Bax, Bcl-2, caspase-3, caspase-9, cleaved caspase-3, cleaved caspase-9, and β-actin. The expression level of total β-actin was used as the loading control (n = 3). Values are mean ± SD. $*P < 0.05$, $**P < 0.01$ compared with the control.

of preadipocytes. We first determined the ratio of phosphorylated IRS-1^{T896}, which showed a higher level in the Foxc2 forced expression group, along with elevated expression of phosphorylation (p)-Akt^{ser473} and p-mTOR^{Ser2448} (Fig. 1A), suggesting that the IRS-1 signaling pathway was involved and activated the Akt and mTOR pathways. Figure 1B shows that the expression of cyclin E and p27 were both elevated in the Foxc2 overexpressed group ($P < 0.05$). To determine whether these effects were affected by Akt signaling, we treated preadipocytes with Akt phosphorylation inhibitor MK2206, and measured phosphorylated Akt^{Ser473} and p-mTOR^{Ser2448}. MK2206 is an allosteric inhibitor of Akt, and it could bind to the Akt kinase domain, which is an allosteric site, resulting in a conformational change, and then block the ATP binding site. Moreover, MK2206 had been used as a selective allosteric inhibitor of Akt phosphorylation (27–29). We found that MK2206 significantly blocked phosphorylation of Akt^{Ser473} and decreased the expression of the cyclin E and p27 ($P < 0.05$) (Fig. 1A, B). Foxc2 overexpression reversed this effect (**Fig. 5A**), while MK2206 had a minor effect on raptor and p-mTOR^{Ser2448} (Fig. 5A). Thus, we determined the levels of p-ERK1/2 and p- mTOR^{Ser2448}. As shown in Fig. 5C, D, Foxc2 increased the levels of p-ERK1/2, p-mTOR^{Ser2448}, and raptor significantly, along with a higher expression of cyclin E, while the addition of ERK phosphorylated inhibitor U0126 blocked the phosphorylated ERK and largely reduced the level of raptor and the phosphorylation of mTOR^{Ser2448}. To further examine the regulation of the upstream pathways of mTORC1, we co-treated preadipocytes with MK2206 and U0126. Forced expression of Foxc2 failed to affect the expression of raptor and p-mTOR^{Ser2448} (Fig. 5E). Because rapamycin treatment can inhibit mTORC1, we used rapamycin as the inhibitor of mTORC1 signaling to determine the role of mTORC1 in the regulation of Foxc2 on preadipocyte proliferation and apoptosis. Figure 5F, G indicates that Foxc2 markedly positively regulated raptor and p27 and negatively regulated caspase-9. Taken together, our data demonstrate that Foxc2 regulates preadipocyte proliferation and apoptosis via both the Akt/mTORC1 pathway and the ERK/mTORC1 pathway.

DISCUSSION

Obesity is determined by the number and volume of adipocytes in adipose tissue, which not only depends on intracellular triglyceride synthesis and catabolic efficiency, but also on the balance between cell proliferation and death, including necrosis and apoptosis (30–34). Cell proliferation is the result of mitosis that is regulated by the cell cycle and requires a variety of regulatory mechanisms to genes, either positively or negatively, to coordinate each other (35–37). Cyclin E is a nuclear protein that can accelerate the cell cycle and enhance the ability of cell

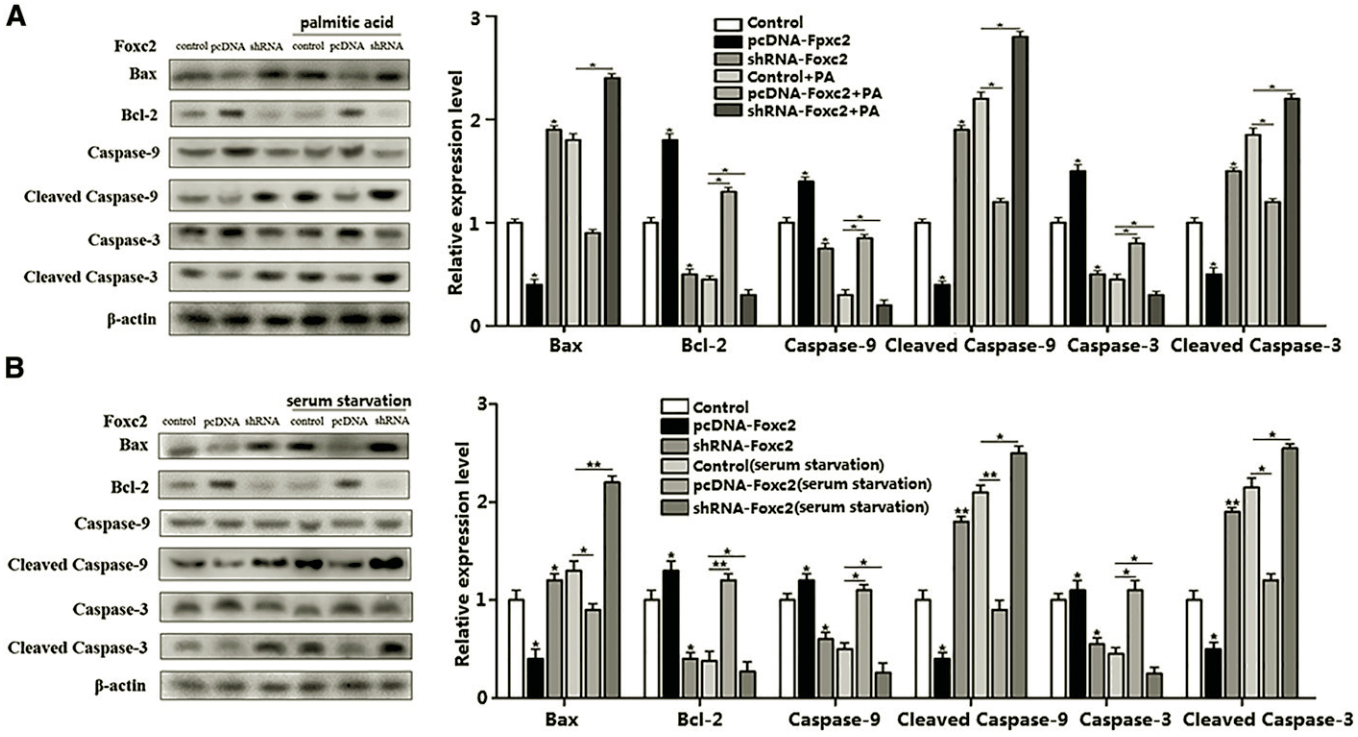

Fig. 4. Foxc2 attenuated serum-starved and palmitate-induced preadipocyte apoptosis. Mouse preadipocytes were pretreated with either pcDNA-Foxc2 or shRNA-Foxc2. A: Protein expression of Bax, Bcl-2, caspase-3, caspase-9, cleaved caspase-3, cleaved caspase-9, and β-actin after treatment with palmitic acid (PA) for 24 h (n = 3). B: Protein expression of Bax, Bcl-2, caspase-3, caspase-9, cleaved caspase-3, cleaved caspase-9, and β-actin after serum starvation treatment for 24 h. The expression level of total β-actin was used as the loading control (n = 3). Values are mean ± SD. $*P < 0.05$ compared with the control.

proliferation, whereas p27 is a negative regulator of cell division, which binds to cyclin and then inhibits the biological activity of complex cyclin-dependent kinase in murine fibroblasts (38, 39). Thus, manipulating the regulatory genes could alter proliferation and apoptosis of adipocytes, offering alternative approaches to prevent obesity. In this study, we found that a HFD significantly induced Foxc2 and cyclin E expression. Foxc2 also inhibited preadipocyte differentiation and increased the cell counts, which is consistent with previous research. Additionally, Foxc2 promoted the expression of positive regulator cyclin E, while it inhibited the expressions of negative regulators p27 and p53. We verified this effect further by cell cycle assay or in a serum-starved model, and obtained consistent results. Our findings suggest that Foxc2 plays a positive regulatory role in cell proliferation by promoting the process of cell cycle transmission in preadipocytes.

Apoptosis of pancreatic β cells induced by fatty acids involves the transcription factor FoxO1 (40), and Foxc1 and Foxc2 play pivotal roles in the early processes of heart development and cardiovascular development (10, 41–43). However, the relationship between Foxc2 and apoptosis of cells remains ambiguous. In this study, we found that shRNA-Foxc2 significantly decreased the mitochondrial membrane potential and increased nuclear genomic DNA fragmentation, whereas Foxc2 expression reversed those effects. Moreover, Foxc2 showed reversal functions on the regulation of activities of genes involved in mitochondrial apoptosis, such as Bcl-2, Bax, caspase-9, and cleaved caspase-9. We applied treatments of serum starvation and palmitic acid to activate caspase-3 and cleaved caspase-3, and then the Foxc2 interference reversed the treatment effects. By TUNEL and annexin-V/PI staining, we showed that the rate of apoptosis was attenuated in Foxc2-forced expression and increased in shRNA-Foxc2 group. These results all indicate that Foxc2 could inhibit preadipocyte apoptosis.

The Akt/mTOR signaling pathway has important functions in cell proliferation and apoptosis, and activation of the Akt/mTOR signaling pathway can promote adipocyte proliferation and inhibit apoptosis (19, 20, 44–46). BSTA could suppress expression of Foxc2 and stimulate adipocyte differentiation, whereas Foxc2 could also promote osteoblast and colorectal cancer proliferation by activation of the Akt signaling pathway. It seems that Akt signaling plays an intricate role in Foxc2 function. In this study, we found that the expression of Foxc2 enhanced the phosphorylation of Akt and the phosphorylation of the Akt substrate, Foxo3a.

Another mechanism that has been implicated in the mechanical activation of mTOR signaling involves signaling by ERK1/2. For example, previous studies have demonstrated that ERK can induce mTOR signaling via the phosphorylation of raptor (21, 47–50). In support of these data, we demonstrated that the expression of Foxc2 enhanced the phosphorylation of the ERK1/2 signaling pathway. Additionally, the mTORC1 pathway key protein raptor, phosphorylation of mTOR, and

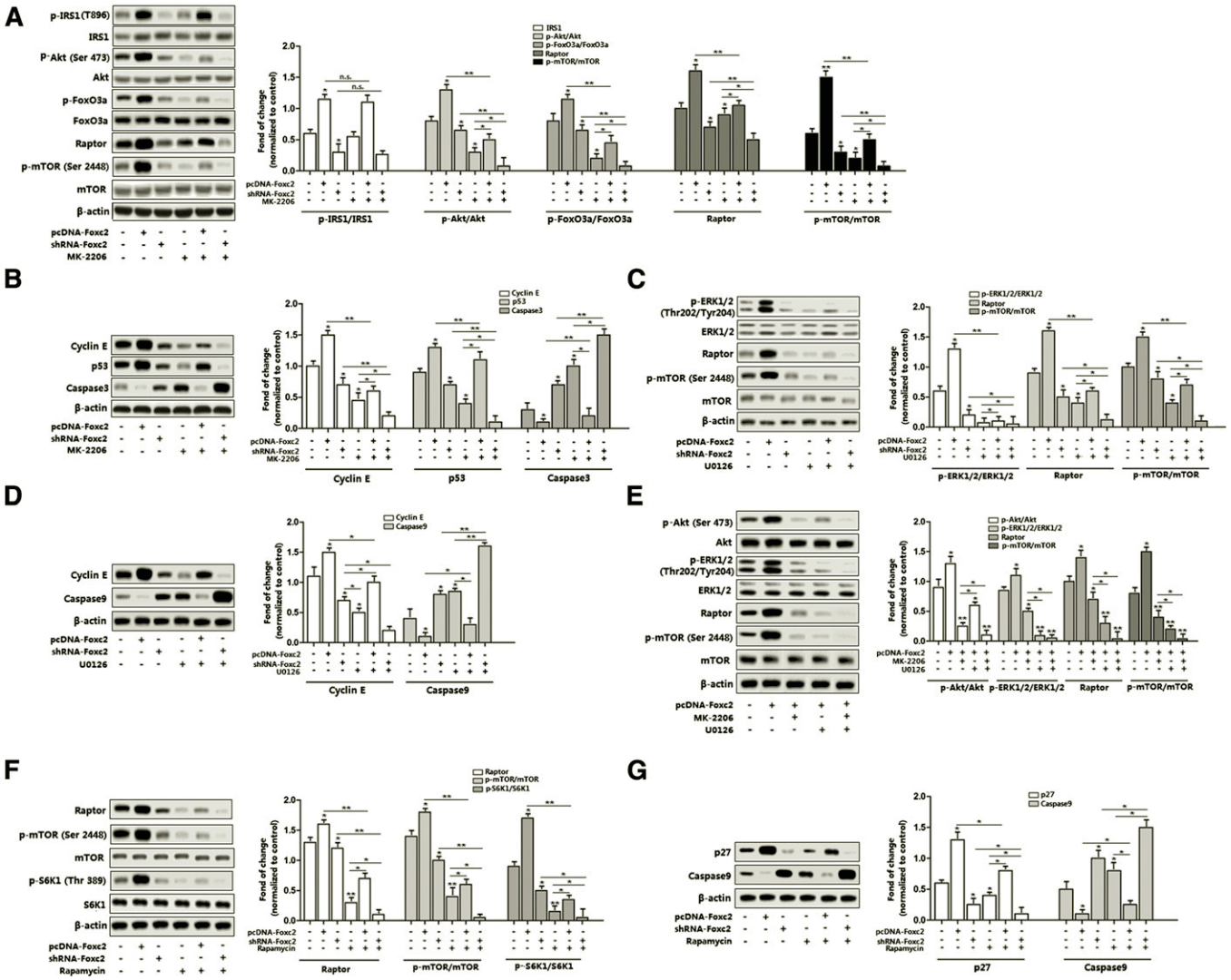

Fig. 5. Foxc2 regulated proliferation and apoptosis of preadipocytes via the mTORC1 pathway. Mouse preadipocytes were pretreated with pcDNA-Foxc2, shRNA-Foxc2, MK-2206, U0126, and rapamycin, respectively. A: Representative immunoblots and densitometric quantification for p-IRS1, p-Akt^{ser473}, p-FoxO3a, and p-mTOR^{Ser2448} (n = 3) with or without MK-2206. B: Representative immunoblots and densitometric quantification for cyclin E, p53, and caspase-3 (n = 3) with or without MK-2206. C: Representative immunoblots and densitometric quantification for p-ERK1/2, raptor, and p-mTOR^{Ser2448} (n = 3) with or without U0126. D: Representative immunoblots and densitometric quantification for cyclin E and caspase-9 (n = 3) with or without U0126. E: Representative immunoblots and densitometric quantification for p-Akt^{Ser473}, p-ERK1/2, raptor, and p-mTOR^{Ser2448} (n = 3) with or without MK-2206 or U0126. F: Representative immunoblots and densitometric quantification for raptor, p-mTOR^{Ser2448}, and p-S6K1^{Thr389} (n = 3) with or without rapamycin. G: Representative immunoblots and densitometric quantification for p27 and caspase-9 (n = 3) with or without rapamycin. The level of total β-actin was used as the loading control. Values are mean ± SD. $*P < 0.05$, $**P < 0.01$ compared with the control.

phosphorylation of S6K1 were activated by Foxc2 and inhibited by rapamycin. The phosphorylation level was attenuated by MK-2206, a highly specific inhibitor to the Akt signaling pathway, and attenuated by rapamycin, a highly specific inhibitor to the mTORC1 signaling pathway. And the same data were detected for adipocytes treated with the specific inhibitor of ERK1/2 signal pathway U0126. Furthermore, when MK-2206 or U0126 was added, we also detected the expression of those genes regulating cell proliferation, such as cyclin E, p53, and p27, and apoptotic key factors caspase-3 and caspase-9. We anticipated that co-treatment with MK-2206 and U0126 would inhibit the mTORC1 signaling pathway, and that they should alleviate the effects of Foxc2 on proliferation promotion and apoptosis inhibition. All these results confirm that Foxc2 functions necessarily via the mTORC1 signaling pathway, which is regulated by the upstream ERK1/2 pathway and partly by the Akt pathway.

CONCLUSION

In conclusion, this study provides a new insight into the regulatory mechanisms of Foxc2 on proliferation and apoptosis of preadipocytes. We further confirmed that the effects of Foxc2 on the proliferation and apoptosis were via the Akt and ERK1/2 pathways and their downstream mTORC1 signaling pathway (**Fig. 6**). Our results would

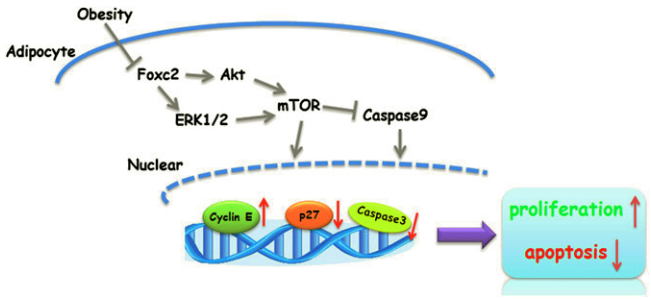

Fig. 6. Summary of the effects of Foxc2 on proliferation and apoptosis of adipocytes. Forced expression of Foxc2 promoted preadipocyte proliferation and inhibited preadipocyte apoptosis via the activation of the Akt/mTORC1 and ERK/mTORC1 signaling pathways.

contribute to the development of novel approaches to prevent and treat obesity and type 2 diabetes.

The authors express their gratitude to Professor Shimin Liu from the University of Western Australia and Professor C. Y. Hu from the University of Hawaii at Manoa for helping to revise the paper.

REFERENCES

1. Bai, X., J. Wang, Y. Guo, J. Pan, Q. Yang, M. Zhang, H. Li, L. Zhang, J. Ma, F. Shi, et al. 2014. Prostaglandin E2 stimulates β1-integrin expression in hepatocellular carcinoma through the EP1 receptor/PKC/NF-κB pathway. *Sci. Rep.* **4:** 6538.
2. Mani, S. A., J. Yang, M. Brooks, G. Schwaninger, A. Zhou, N. Miura, J. L. Kutok, K. Hartwell, A. L. Richardson, and R. A. Weinberg. 2007. Mesenchyme forkhead 1 (FOXC2) plays a key role in metastasis and is associated with aggressive basal-like breast cancers. *Proc. Natl. Acad. Sci. USA.* **104:** 10069–10074.
3. Töpf, A., H. R. Griffin, E. Glen, R. Soemedi, D. L. Brown, D. Hall, T. J. Rahman, J. J. Eloranta, C. Jüngst, and A. G. Stuart. 2014. Functionally significant, rare transcription factor variants in tetralogy of Fallot. *PLoS One.* **9:** e95453.
4. Kume, T., K. Deng, and B. Hogan. 2000. Murine forkhead/winged helix genes Foxc1 (Mf1) and Foxc2 (Mfh1) are required for the early organogenesis of the kidney and urinary tract. *Development.* **127:** 1387–1395.
5. Håkansson, J., B. Eliasson, U. Smith, and S. Enerbäck. 2011. Adipocyte mitochondrial genes and the forkhead factor FOXC2 are decreased in type 2 diabetes patients and normalized in response to rosiglitazone. *Diabetol. Metab. Syndr.* **3:** 32.
6. Cederberg, A., L. M. Grønning, B. Ahrén, K. Taskén, P. Carlsson, and S. Enerbäck. 2001. FOXC2 is a winged helix gene that counteracts obesity, hypertriglyceridemia, and diet-induced insulin resistance. *Cell.* **106:** 563–573.
7. Davis, K. E., M. Moldes, and S. R. Farmer. 2004. The forkhead transcription factor FoxC2 inhibits white adipocyte differentiation. *J. Biol. Chem.* **279:** 42453–42461.
8. Zhang, J., Y. Zhang, T. Sun, F. Guo, S. Huang, M. Chandalia, N. Abate, D. Fan, H. B. Xin, and Y. E. Chen. 2013. Dietary obesity-induced Egr-1 in adipocytes facilitates energy storage via suppression of FOXC2. *Sci. Rep.* **3:** 1476.
9. Lidell, M. E., E. L. Seifert, R. Westergren, M. Heglind, A. Gowing, V. Sukonina, Z. Arani, P. Itkonen, S. Wallin, and F. Westberg. 2011. The adipocyte-expressed forkhead transcription factor Foxc2 regulates metabolism through altered mitochondrial function. *Diabetes.* **60:** 427–435.
10. Seo, S., and T. Kume. 2006. Forkhead transcription factors, Foxc1 and Foxc2, are required for the morphogenesis of the cardiac outflow tract. *Dev. Biol.* **296:** 421–436.
11. Yao, Y., M. Suraokar, B. G. Darnay, B. G. Hollier, T. E. Shaiken, T. Asano, C. H. Chen, B. H. Chang, Y. Lu, and G. B. Mills. 2013. BSTA promotes mTORC2-mediated phosphorylation of Akt1 to suppress expression of FoxC2 and stimulate adipocyte differentiation. *Sci. Signal.* **6:** ra2.
12. Grønning, L. M., A. Cederberg, N. Miura, S. Enerbäck, and K. Taskén. 2002. Insulin and TNFα induce expression of the forkhead transcription factor gene Foxc2 in 3T3–L1 adipocytes via PI3K and ERK 1/2-dependent pathways. *Mol. Endocrinol.* **16:** 873–883.
13. Kim, J. K., H. J. Kim, S. Y. Park, A. Cederberg, R. Westergren, D. Nilsson, T. Higashimori, Y. R. Cho, Z. X. Liu, and J. Dong. 2005. Adipocyte-specific overexpression of FOXC2 prevents diet-induced increases in intramuscular fatty acyl CoA and insulin resistance. *Diabetes.* **54:** 1657–1663.
14. Hader, C., A. Marlier, and L. Cantley. 2010. Mesenchymal-epithelial transition in epithelial response to injury: the role of Foxc2. *Oncogene.* **29:** 1031–1040.
15. Gozo, M. C., P. J. Aspuria, D. J. Cheon, A. E. Walts, D. Berel, N. Miura, B. Y. Karlan, and S. Orsulic. 2013. Foxc2 induces Wnt4 and Bmp4 expression during muscle regeneration and osteogenesis. *Cell Death Differ.* **20:** 1031–1042.
16. Omoteyama, K., Y. Mikami, and M. Takagi. 2007. Foxc2 induces expression of MyoD and differentiation of the mouse myoblast cell line C2C12. *Biochem. Biophys. Res. Commun.* **358:** 885–889.
17. Marie, P. J. 2013. Targeting integrins to promote bone formation and repair. *Nat. Rev. Endocrinol.* **9:** 288–295.
18. Kim, S. W., S. M. Kim, H. Bae, D. Nam, J. H. Lee, S. G. Lee, B. S. Shim, S. H. Kim, K. S. Ahn, and S. H. Choi. 2013. Embelin inhibits growth and induces apoptosis through the suppression of Akt/mTOR/S6K1 signaling cascades. *Prostate.* **73:** 296–305.
19. Markman, B., R. Dienstmann, and J. Tabernero. 2010. Targeting the PI3K/Akt/mTOR pathway-beyond rapalogs. *Oncotarget.* **1:** 530–543.
20. Scott, P. H., G. J. Brunn, A. D. Kohn, R. A. Roth, and J. C. Lawrence. 1998. Evidence of insulin-stimulated phosphorylation and activation of the mammalian target of rapamycin mediated by a protein kinase B signaling pathway. *Proc. Natl. Acad. Sci. USA.* **95:** 7772–7777.
21. Kohno, M., and J. Pouyssegur. 2006. Targeting the ERK signaling pathway in cancer therapy. *Ann. Med.* **38:** 200–211.
22. Wang, Y., M. Sato, Y. Guo, T. Bengtsson, and J. Nedergaard. 2014. Protein kinase A-mediated cell proliferation in brown preadipocytes is independent of Erk1/2, PI3K and mTOR. *Exp. Cell Res.* **328:** 143–155.
23. Wang, C., and R. J. Youle. 2009. The role of mitochondria in apoptosis. *Annu. Rev. Genet.* **43:** 95–118.
24. Listenberger, L. L., D. S. Ory, and J. E. Schaffer. 2001. Palmitate-induced apoptosis can occur through a ceramide-independent pathway. *J. Biol. Chem.* **276:** 14890–14895.
25. Martinez, S. C., K. Tanabe, C. Cras-Méneur, N. A. Abumrad, E. Bernal-Mizrachi, and M. A. Permutt. 2008. Inhibition of Foxo1 protects pancreatic islet β-cells against fatty acid and endoplasmic reticulum stress-induced apoptosis. *Diabetes.* **57:** 846–859.
26. Mu, Y. M., T. Yanase, Y. Nishi, A. Tanaka, M. Saito, C. H. Jin, C. Mukasa, T. Okabe, M. Nomura, and K. Goto. 2001. Saturated FFAs, palmitic acid and stearic acid, induce apoptosis in human granulosa cells. *Endocrinology.* **142:** 3590–3597.
27. Rehan, M., M. A. Beg, S. Parveen, G. A. Damanhouri, and G. F. Zaher. 2014. Computational insights into the inhibitory mechanism of human AKT1 by an orally active inhibitor, MK-2206. *PLoS One.* **9:** e109705.
28. Hirai, H., H. Sootome, Y. Nakatsuru, K. Miyama, S. Taguchi, K. Tsujioka, Y. Ueno, H. Hatch, P. K. Majumder, and B. S. Pan. 2010. MK-2206, an allosteric Akt inhibitor, enhances antitumor efficacy by standard chemotherapeutic agents or molecular targeted drugs in vitro and in vivo. *Mol. Cancer Ther.* **9:** 1956–1967.
29. Tan, S., Y. Ng, and D. James. 2011. Next-generation Akt inhibitors provide greater specificity: effects on glucose metabolism in adipocytes. *Biochem. J.* **435:** 539–544.
30. Butler, A. E., J. Janson, S. Bonner-Weir, R. Ritzel, R. A. Rizza, and P. C. Butler. 2003. β-cell deficit and increased β-cell apoptosis in humans with type 2 diabetes. *Diabetes.* **52:** 102–110.
31. Francés, D. E., O. Motino, N. Agra, A. Gonzalez-Rodriguez, A. Fernandez-Alvarez, C. Cucarella, R. Mayoral, L. Castro-Sanchez, E. Garcia-Casarrubios, L. Bosca, et al. 2015. Hepatic cyclooxygenase-2 expression protects against diet-induced steatosis, obesity and insulin resistance. *Diabetes.* **64:** 1522–1531.
32. Furukawa, S., T. Fujita, M. Shimabukuro, M. Iwaki, Y. Yamada, Y. Nakajima, O. Nakayama, M. Makishima, M. Matsuda, and I.

Shimomura. 2004. Increased oxidative stress in obesity and its impact on metabolic syndrome. *J. Clin. Invest.* **114:** 1752–1761.
33. Goodwin, P. J., and V. Stambolic. 2015. Impact of the obesity epidemic on cancer. *Annu. Rev. Med.* **66:** 281–296.
34. Razavi, R., H. S. Najafabadi, S. Abdullah, S. Smukler, M. Arntfield, and D. van der Kooy. 2015. Diabetes enhances the proliferation of adult pancreatic multipotent progenitor cells and biases their differentiation to more β-cell production. *Diabetes.* **64:** 1311–1323.
35. Antonsson, B., and J. C. Martinou. 2000. The Bcl-2 protein family. *Exp. Cell Res.* **256:** 50–57.
36. Vander Heiden, M. G., L. C. Cantley, and C. B. Thompson. 2009. Understanding the Warburg effect: the metabolic requirements of cell proliferation. *Science.* **324:** 1029–1033.
37. Harper, J. W., G. R. Adami, N. Wei, K. Keyomarsi, and S. J. Elledge. 1993. The p21 Cdk-interacting protein Cip1 is a potent inhibitor of G1 cyclin-dependent kinases. *Cell.* **75:** 805–816.
38. Minella, A. C., K. R. Loeb, A. Knecht, M. Welcker, B. J. Varnum-Finney, I. D. Bernstein, J. M. Roberts, and B. E. Clurman. 2008. Cyclin E phosphorylation regulates cell proliferation in hematopoietic and epithelial lineages in vivo. *Genes Dev.* **22:** 1677–1689.
39. Sheaff, R. J., M. Groudine, M. Gordon, J. M. Roberts, and B. E. Clurman. 1997. Cyclin E-CDK2 is a regulator of p27Kip1. *Genes Dev.* **11:** 1464–1478.
40. Lin, H. Y., Y. Yin, J. X. Zhang, H. Xuan, Y. Zheng, S. S. Zhan, Y. . Zhu, and X. Han. 2012. Identification of direct forkhead box O1 targets involved in palmitate-induced apoptosis in clonal insulin-secreting cells using chromatin immunoprecipitation coupled to DNA selection and ligation. *Diabetologia.* **55:** 2703–2712.
41. Bell, A., A. Gagnon, P. Dods, D. Papineau, M. Tiberi, and A. Sorisky. 2002. TSH signaling and cell survival in 3T3-L1 preadipocytes. *Am. J. Physiol. Cell Physiol.* **283:** C1056–C1064.
42. Guo, W., S. Wong, W. Xie, T. Lei, and Z. Luo. 2007. Palmitate modulates intracellular signaling, induces endoplasmic reticulum stress, and causes apoptosis in mouse 3T3–L1 and rat primary preadipocytes. *Am. J. Physiol. Endocrinol. Metab.* **293:** E576–E586.
43. Skrzypski, M., P. Kaczmarek, T. Le, T. Wojciechowicz, E. P. Oszmalek, D. Szczepankiewicz, M. Sassek, A. Arafat, B. Wiedenmann, and K. Nowak. 2012. Effects of orexin A on proliferation, survival, apoptosis and differentiation of 3T3-L1 preadipocytes into mature adipocytes. *FEBS Lett.* **586:** 4157–4164.
44. Bhattacharya, I., and A. Ullrich. 2006. Endothelin-1 inhibits adipogenesis: role of phosphorylation of Akt and ERK1/2. *FEBS Lett.* **580:** 5765–5771.
45. Chuang, C. C., R. S. Yang, K. S. Tsai, F. M. Ho, and S. H. Liu. 2007. Hyperglycemia enhances adipogenic induction of lipid accumulation: involvement of extracellular signal-regulated protein kinase 1/2, phosphoinositide 3-kinase/Akt, and peroxisome proliferator-activated receptor γ signaling. *Endocrinology.* **148:** 4267–4275.
46. Reusch, J. E., and D. J. Klemm. 2002. Inhibition of cAMP-response element-binding protein activity decreases protein kinase B/Akt expression in 3T3-L1 adipocytes and induces apoptosis. *J. Biol. Chem.* **277:** 1426–1432.
47. Miyazaki, M., J. J. McCarthy, M. J. Fedele, and K. A. Esser. 2011. Early activation of mTORC1 signaling in response to mechanical overload is independent of phosphoinositide 3-kinase/Akt signaling. *J. Physiol.* **589:** 1831–1846.
48. Ma, L., Z. Chen, H. Erdjument-Bromage, P. Tempst, and P. P. Pandolfi. 2005. Phosphorylation and functional inactivation of TSC2 by Erk: implications for tuberous sclerosis and cancer pathogenesis. *Cell.* **121:** 179–193.
49. Roux, P. P., B. A. Ballif, R. Anjum, S. P. Gygi, and J. Blenis. 2004. Tumor-promoting phorbol esters and activated Ras inactivate the tuberous sclerosis tumor suppressor complex via p90 ribosomal S6 kinase. *Proc. Natl. Acad. Sci. USA.* **101:** 13489–13494.
50. Carriere, A., Y. Romeo, H. A. Acosta-Jaquez, J. Moreau, E. Bonneil, P. Thibault, D. C. Fingar, and P. P. Roux. 2011. ERK1/2 phosphorylate raptor to promote Ras-dependent activation of mTOR complex 1 (mTORC1). *J. Biol. Chem.* **286:** 567–577.